

Stephen Durden, Eastwood Im, Fuk Li, Amarit Kitiyakara, Alan Tanner, and William Wilson

Jet Propulsion Laboratory
 California Institute of Technology
 Pasadena, CA 91109, USA

T: (818) 354-4719 F: (818) 393-5285 EMail: durden@fringe.jpl.nasa.gov

ABSTRACT

The NASA/JPL Airborne Rain Mapping Radar (ARMAR) was deployed for rainfall observations during TOGA/COARE on the NASA DC-8 aircraft. A total of ~30 hours of rain profiling measurements were collected over the Western Pacific Ocean during January and February 1993. The rain systems observed included isolated convective cells, mesoscale convective complexes, and a tropical cyclone.

Our preliminary results show that the radar bright bands of the observed stratiform rain were typically located at or above 4.5 km, although occasionally some appeared at altitudes as low as 4.1 km. Our results also show relatively large reflectivity variations in stratiform rain. In our rain attenuation study, we show that the radar surface reference technique and the radiometer technique produce similar path-integrated attenuation estimates for one-way attenuations ≤ 4 dB. The radar technique, however, has the potential of providing accurate estimates at larger attenuations when the radiometer is saturated. The dual-polarization radar profiling measurements show that the local extrema of Z_{DR} , ρ_{hv} , ϕ_{hv} occurred near the bottom of the melting layer. These extrema were probably caused by the presence of varying mixture of hydrometeors with various shape, size, and thermodynamic phase.

1. INTRODUCTION

The NASA/JPL Airborne Rain Mapping Radar (ARMAR) has been developed for the purpose of supporting future spaceborne rain radar systems, including the radar for the Tropical Rainfall Measuring Mission (TRMM), to be flown in the late 1990's. ARMAR flies on the NASA Ames DC-8 aircraft and measures reflectivity at the TRMM radar frequency of 13.8 GHz. It operates in a downward looking, cross-track scanning geometry. During normal operation at an altitude of 12 Km, ARMAR can acquire measurements over a cross-track surface swath of 10 Km at a horizontal resolution of 800 m and a vertical resolution of 60 m. In addition to acquiring single-polarization rain reflectivity measurements, ARMAR can also be configured to acquire dual-polarization and Doppler radar measurements as well as brightness temperature measurements. The key system and performance characteristics of ARMAR are shown in Table 1. Further details on the ARMAR design can be found in Durden *et al.* (1994) and Tanner *et al.* (1994).

| | |
|--|----------------|
| Operating Frequency | 13.8 GHz |
| Surface Horizontal Resolution | 800 m |
| Vertical Resolution | 60 m |
| Polarization | HH, Vv, Hv |
| Antenna Beamwidth | 3.8° |
| Antenna Scan Angle | $\pm 20^\circ$ |
| Transmitter Power | 200 w |
| Transmit Chirp Pulse Duration | 5-45 μ sec |
| Chirp Bandwidth | 4 MHz |
| Pulse Repetition Frequency | 1-8 KHz |
| Analog-to-Digital Sampling Rate | 10 MHz |
| Analog-to-Digital Converter Resolution | 12 bits |

Table 1. ARMAR system characteristics.

ARMAR participated in all 13 flights of the NASA DC-8 in the Tropical Ocean Global Atmosphere - Coupled Ocean-Atmosphere Response Experiment (TOGA/COARE) over the Western Pacific

Ocean in January and February of 1993 and acquired approximately 30 hours of rain data. This data set represents tropical rainfall systems ranging from isolated convective cells to large anvil systems and tropical cyclones. In this paper, we discuss a number of features of the observed stratiform rain systems, include the radar bright band height and reflectivity. We also compare some path-integrated rain attenuation results that we have obtained using the ARMAR radar reflectivity measurements versus those obtained using the radiometer brightness temperature measurements. Finally, we summarize some preliminary results on the dual-polarized reflectivity measurements.

2. BRIGHT BAND HEIGHT AND REFLECTIVITY

While most of our data were acquired over convective systems, much of the observed rainfall was actually the stratiform rain associated with these systems. Our observations of the stratiform rain in TOGA/COARE show that it was quite variable in both the horizontal and vertical dimensions. Within the melting layer the melting aggregates have radar reflectivity that is higher than that of the rain below. Therefore, this region is often being referred to as the radar bright band (Battan, 1975). From the ARMAR TOGA/COARE data, we compiled the bright band height and reflectivity information for the stratiform rain with well-defined melting layers, in Fig. 1 we show the distribution of the bright band heights. In this figure, the bright band height corresponds to the altitude within the radar range profile at which the radar reflectivity is the highest (excluding the surface returns), and the count corresponds to the number of radar profiles collected at a constant echo reception rate along the DC-8 flight path. Out of a total of 9089 measurements used in Fig. 1, 61% of the bright band heights were 4.5 km or above, 32% were between 4.3 and 4.5 km. and 7% were below 4.3 km.

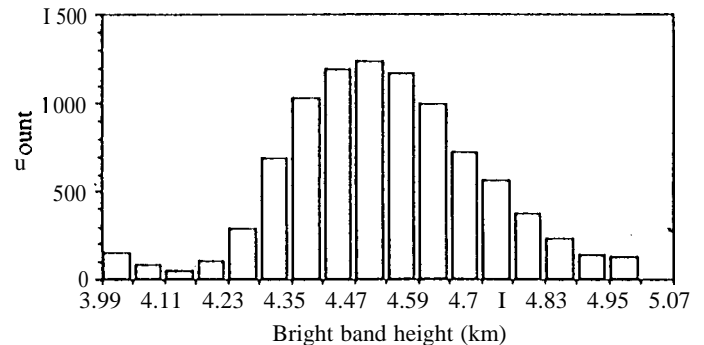


Figure 1. Distribution of the bright band height measured by ARMAR at nadir viewing during TOGA/COARE.

In Fig. 2, we show two distributions of the corresponding radar bright band reflectivity measured by ARMAR. The shaded reflectivity distribution is for bright bands with heights below 4.3 km, and the unshaded reflectivity distribution is for bright bands with heights above 4.3 km. Significant variations in the radar bright band reflectivity can be seen in each of these two distributions. It is also interesting to note that a significant portion (35%) of the low-altitude bright bands (< 4.3 km) had reflectivity values above 42 dBZ, whereas only 11 % of the higher-altitude bright bands had reflectivity values above 42 dBZ. One possible speculation for the observed high reflectivity with bright bands at lower altitude is that

some underlying convective updrafts might have held up sufficient amount of melting particles, which in turn produced a maximum radar reflectivity at a location below the true bright band.

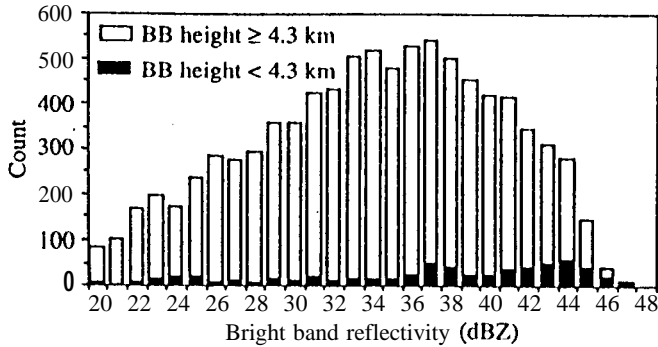


Figure 2. Distributions of the maximum reflectivity of the bright band measured by ARMAR at nadir during TOGA/COARE.

3. ESTIMATION OF PATH-INTEGRATED ATTENUATION

The path-integrated attenuation (*PIA*) provides an estimate of the path-integrated rainfall rate (Meneghini *et al.*, 1983) and is also useful as a constraint in some rain rate profiling algorithms (e.g., Meneghini and Nakamura, 1990; Marzoug and Amayenc, 1991). In this section, we compare the use of the radar surface reference technique (Meneghini *et al.*, 1983) with the use of the radiometer brightness temperature to estimate attenuation. For this study we have examined 15 flight legs acquired during 12 different flights. This corresponds to 2781 measurements in rainfall. Each radar measurement consists of an average of approximately 100 independent samples, giving a radar measurement standard deviation of approximately ± 0.5 dB. Each radiometer measurement has a precision of about 1 K.

For the radar approach, we examined the nadir surface cross section throughout each selected flight leg. To estimate *PIA*, the surface cross section of each rain area was subtracted from the reference cross section measured in the closest preceding clear area, where the clear areas were defined as having brightness temperatures < 152 K at 13.8 GHz. The average attenuation on our clear area measurements, which was estimated to be 0.4 dB, was added to the estimated *PIA* in order to remove the bias.

Estimation of *PIA* using the nadir-viewing radiometer measurement is more complicated. For a single-frequency radiometer, accurate estimates of attenuation can only be made when the brightness temperature is well below the saturation temperature, where scattering is a minor contribution. Here, we used a simple radiative transfer model (Fujita *et al.*, 1985) to compute the brightness temperature (T_b) for a variety of attenuation profiles, and derived an inversion relationship by fitting the data that were below the saturation temperature with a quadratic function. The resulting relationship is

$$PIA_{mr} = 0.34 + 0.000192 (T_b - 125)^2$$

where the subscript *mr* stands for microwave radiometer. This fit is quite accurate, yielding a correlation coefficient of 0.97,

Fig. 3 shows an example of the radar and radiometer derived attenuations along a single 10-minute flight leg on February 8, 1993. The two estimates are in general quite close but there are a few points where the radar estimate is much higher than the radiometer estimate. Fig. 4 shows the radar estimated *PIA* versus the radiometer estimated *PIA* for all 15 flight legs. For *PIAs* less than about 4 dB, the two estimates agree. We note that of the 2781 measurements, 223 of them have radiometer attenuations less than 4 dB, so the two methods agree for 80% of our data. The mean difference between the two estimates is only 0.06 dB, and the rms difference is 0.7 dB. We believe that the rms difference is primarily due to fluctuations in the surface wind and hence the radar estimate. Since a modification

of the surface by rainfall would be expected to produce a bias in the radar technique, these data suggest that the effect of rain modifications is small at low attenuations and rain rates. For attenuations greater than 4 dB as measured by the radiometer (20% of our data), the radar attenuation can be up to 25 dB. For these large attenuations the radiometer is saturated; attenuations of 5 dB and 25 dB yield nearly the same brightness temperature.

The *PIA* measurements can be converted to a path-averaged rain rate using $k = 0.03R$ (Olsen *et al.*, 1978), where k is the rain absorption coefficient in dB/km and R is the rain rate in mm/h. By assuming that the attenuation occurs over a 4.5 km path, the path-averaged rain rate in mm/h is 7.4 times the *PIA* in dB. Thus, according to the radar technique, path-averaged rain rates of well over 100 mm/h were observed on a number of occasions. High surface winds in convective storms could have reduced the nadir surface cross section, causing the surface reference technique to overestimate the *PIA* by several decibels. Even if this is the case, the *PIA* in several cases is at least 15 dB, corresponding to path-averaged rain rates in excess of 100 mm/h.

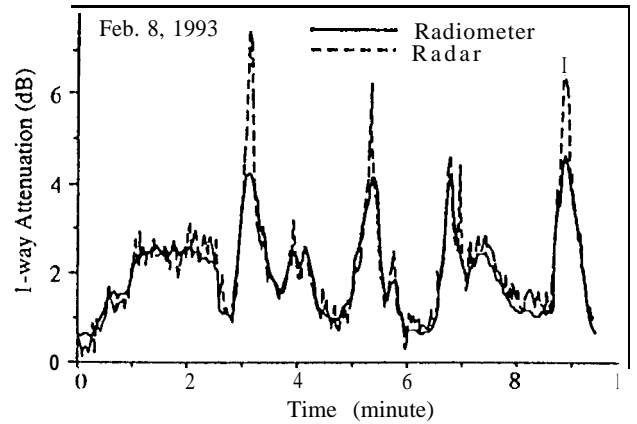


Figure 3. Example of radar and radiometer attenuations over a 10-minute period along a single flight leg at nadir. Data was acquired on February 8, 1993.

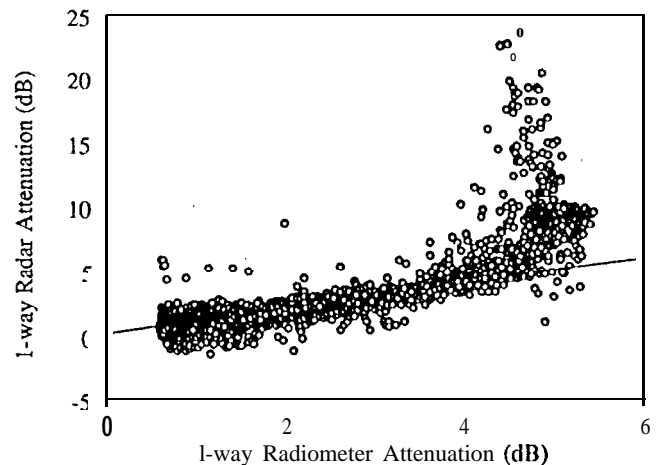


Figure 4. The measured radar *PIA* versus the measured radiometer *PIA* for 15 flight legs in TOGA/COARE at nadir incidence.

4. DUAL-POLARIZATION MEASUREMENTS

We have examined some dual-polarization radar data acquired over stratiform rain. In Figure 5 we show an example of the deduced dual-polarization rain parameters and compare them with the single-polarization reflectivity and Doppler measurements. The data shown here were collected by ARMAR on January 19, 1993 using an

alternating horizontal-polarization and vertical-polarization sequence at 30° off-nadir. The processed parameters include horizontally-polarized reflectivity factor (Z_h), radial rainfall velocity (V), differential reflectivity (Z_{DR}), co-polar correlation coefficient (ρ_{hv}), and differential phase (ϕ_{hv}).

The profile of Z_h depicts a typical bright band with a layer of reflectivity above 30 dBZ. Due to the pulse smearing at 30° incidence, the bright band appears less distinct and its thickness stretches over a greater extent. The rainfall velocity goes from 0-1 m/s at the top of the bright band and it accelerates to 6 m/s over the width of the bright band. These Z_h and V profiles are consistent with the facts that the melting of the large ice aggregates to large rain drops causes the increase in reflectivity and that the acceleration of the drops downward causes the decrease in reflectivity.

The dual-polarized rain parameter profiles (Z_{DR} , ρ_{hv} , ϕ_{hv}) all have local extrema near the bottom of the melting layer. We have also observed similar signatures for measurements obtained in other TOGA/COARE flight legs. Note that the differential phase contributed by the forward aircraft motion is about -47°. Hence, the maximum backscatter differential phase in this example is about -3°. By comparing these results with the simulated results obtained by Zmic et al., (1993) using both oblate and prolate spheroid scattering models at 4 GHz, the relatively large differential phase maximum and the corresponding Z_{DR} value are probably due to scattering from oblate rain drops with axis ratios less than 0.3, and the relatively small decrease in correlation is probably due to the presence of larger rain drops. In this example, we also observe that the ϕ_{hv} minimum is located approximately 100 m higher than the extrema of Z_{DR} and ρ_{hv} . A possible explanation for this difference is the presence of larger, less oblate rain drops at an altitude slightly below the ϕ_{hv} minimum. These large drops cause the continuous increase in differential reflectivity and limit the decrease in correlation coefficient.

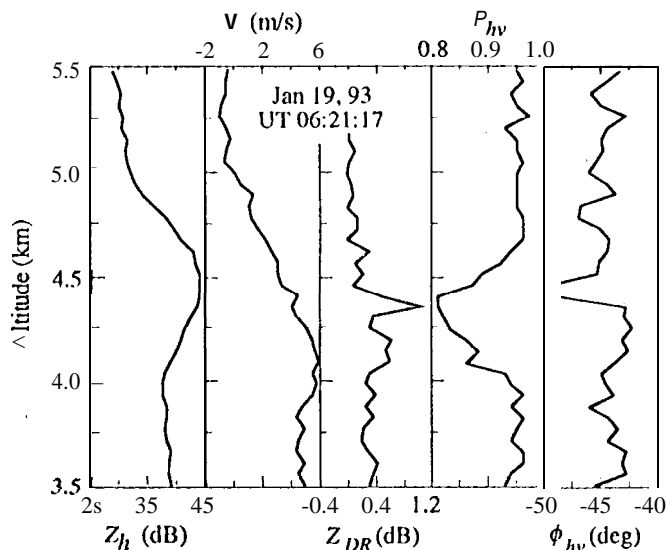


Figure 5. Vertical profiles of horizontal-polarized reflectivity factor (Z_h), radial fall velocity (V), differential reflectivity (Z_{DR}), co-polar correlation coefficient (ρ_{hv}), and differential phase (ϕ_{hv}) obtained by ARMAR at 30° incidence during January 19, 1993.

SUMMARY

The NASA/JPL Airborne Rain Mapping Radar (ARMAR) was deployed during TOGA/COARE on the NASA DC-8 aircraft. ARMAR is a 14 GHz, downward looking radar designed to simulate the TRMM radar frequency and geometry. It can acquire data in a variety of modes, including Doppler and dual-polarization radar

modes, and radiometer mode. A total of 13 flights over the Western Pacific Ocean were made during January and February 1993. The rain systems observed included isolated convective cells, mesoscale convective complexes, and a tropical cyclone. In this paper, we discuss some general features of the observed rainfall systems, and we apply ARMAR data to retrieve some geophysical and electromagnetic characteristics of these systems.

Our TOGA/COARE observations show that the bright bands of the stratiform rain are typically located at or above 4.5 km, although occasionally they appear at altitudes as low as 4.1 km. Quite a number of our stratiform rain observations also show relatively large variations in radar reflectivity.

Using the ARMAR's radar and radiometer data, we show that the radar surface reference technique produces path-integrated attenuation estimates very close to those obtained using radiometer technique for out-way attenuations of approximately 4 dB or less. The radar technique, however, has the potential of providing accurate estimates at large attenuations when the radiometer becomes saturated.

Using the ARMAR's dual-polarization radar profiles, we show that Z_{DR} , ρ_{hv} , ϕ_{hv} have local extrema near the bottom of the melting layer. These extrema are probably caused by the presence of varying mixture of hydrometers with various shape, size, and thermodynamic phase.

ACKNOWLEDGMENT

The research described here was performed by the Jet Propulsion Laboratory, California Institute of Technology, under contract with NASA.

REFERENCES

- Battan, L. J., Radar Observation of the Atmosphere. Univ. of Chicago Press, Chicago, Ill.; p. 324, 1975.
- Durden, S. L., E. Im, F. K. Li, W. Ricketts, A. Tanner, and W. Wilson, "ARMAR: An airborne rain mapping radar," *J. Atmos. Oceanic Tech.*, in press, 1994.
- Fujita, M., K. Okamoto, H. Masuko, T. Ojima, and N. Fugono, "Quantitative measurements of path-integrated rain rate by an airborne microwave radiometer over the ocean," *J. Atmos. Oceanic Tech.*, 2, pp. 285-292, 1985.
- Marzoug, M., and P. Amayenc, "improved range profiling algorithm of rainfall rate from a spaceborne radar with path-integrated attenuation constraint," *IEEE Trans. Geosci. Remote Sensing*, 29, pp. 584-592, 1991.
- Meneghini, R. and K. Nakamura, "Range profiling of the rain rate by an airborne weather radar," *Remote Sens. Environ.*, 31, pp. 193-209, 1990.
- Meneghini, R., J. Eckerman, and D. Atlas, "Determination of rain rate from a spaceborne radar using measurements of total attenuation," *IEEE Trans. Geosci. Remote Sensing*, 20, pp. 34-43, 1983.
- Olsen, R. L., D. V. Rodgers, and D. B. Hodge, "The aR^b relation in the calculation of rain attenuation," *IEEE Trans. Antennas Propagat.*, 26, pp. 318-329, 1978.
- Tanner, A., S. L. Durden, R. Denning, E. Im, F. K. Li, W. Ricketts, and W. Wilson, "Pulse compression with very low sidelobes in an airborne rain mapping radar," *IEEE Trans. Geosci. & Remote Sensing*, in press, 1994.
- Zmic, D. S., N. Balakrishnan, A. Ryzhkov, and S. L. Durden, "Use of co-polar correlation coefficient for precipitation at nearly vertical incidence," *IEEE Trans. Geosci. & Remote Sensing*, submitted, 1993.